Wind Noise Source Characterization and How It Can Be Used To Predict Vehicle Interior Noise

2014-01-2052
Published 06/30/2014

Denis Blanchet and Anton Golota
ESI GmbH

Nicolas Zerbib and Lassen Mebarek
ESI Group

CITATION: Blanchet, D., Golota, A., Zerbib, N., and Mebarek, L., "Wind Noise Source Characterization and How It Can Be Used To Predict Vehicle Interior Noise," SAE Technical Paper 2014-01-2052, 2014, doi:10.4271/2014-01-2052.

Abstract

Recent developments in the prediction of the contribution of wind noise to the interior SPL have opened a realm of new possibilities in terms of i) how the convective and acoustic sources terms can be identified, ii) how the interaction between the source terms and the side glass can be described and finally iii) how the transfer path from the sources to the interior of the vehicle can be modelled. This paper discusses in detail these three aspects of wind noise simulation and recommends appropriate methods to deliver required results at the right time based on i) simulation and experimental data availability, ii) design stage and iii) time available to deliver these results. Several simulation methods are used to represent the physical phenomena involved such as CFD, FEM, BEM, FE/SEA Coupled and SEA. Furthermore, a 1D and 2D wavenumber transformation is used to extract key parameters such as the convective and the acoustic component of the turbulent flow from CFD and/or experimental data whenever available. This paper focuses on process implementation and presents simulation results from coarse to detailed simulation models and compares these with experimental data.

Introduction

In order to model wind noise it is necessary to understand the source, the paths which typically involve direct vibro-acoustic transmission through certain regions of the structure, transmission through nearby leaks/seals and isolation and absorption provided by the interior sound package and the receiver and in particular, the frequency range(s) in which wind noise provides an audible contribution to the interior noise in the occupant's ears. While many regions of a vehicle can contribute to wind noise, the fluctuating surface pressures on the front side glass due to vortices and separated flow generated by the A-pillar and mirror are often an important contributor.

This paper presents an overview of different approaches that can be used to efficiently predict wind noise contribution to overall SPL at the driver's ear. After describing the physical phenomena involved in wind noise simulation, a review of major wind noise source characterization will be presented. Following is a description of vibro-acoustics methods used to predict interior SPL for a given wind noise source model. Topics such as availability of source data, model building and computation time as factors guiding selection of an approach that ensures getting the right model at the right time are then discussed. Finally, validation cases for both vibro-acoustics (VA) and Aero-Vibro-Acoustics (AVA) are presented.

From Turbulent Flow to Vehicle Interior SPL

Physical Phenomena Involved

A turbulent flow generated outside a vehicle contains both a convective and an acoustic pressure fluctuations component on side glass (Figure 1). This energy can potentially be transmitted to the interior of a vehicle and be detrimental to the sound quality experienced by occupants.

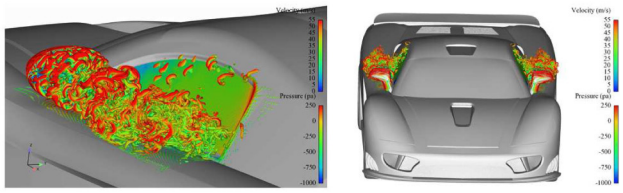

Figure 1. Turbulent flow generated behind side mirror and A-pillar

The following sections describe the main noise generation principles involved in wind noise.

Pressure Fluctuation on Side Glass

The turbulent flow outside a vehicle generates a fluctuating surface pressure field on the side glass which includes a convective and an acoustic component. The convective component is related to the pressure field generated by eddies travelling at the convection speed. The acoustic component is related to acoustic waves travelling within the flow and being generated on various surfaces before reaching the side glass. The acoustic component is typically very small in amplitude compared to the convective component and as will be shown later in this paper, can be the major contributor at coincidence frequency of the side glass. Furthermore, the acoustic waves reaching the side glass are highly directional. Both the convective and the acoustic components contribute to the sound pressure level (SPL) at the driver's ear (Figure 2).

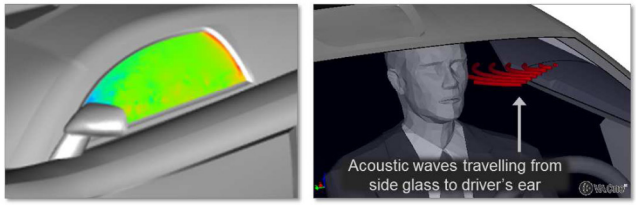

Figure 2. Fluctuating surface pressure on side glass (left) and acoustic waves propagating from side glass to the driver's ear (right).

Pressure Fluctuation on Mirror

In Figure 3 on the left side, the pressure is the highest in the front of the side mirror. It is also the location of lowest fluctuation. The flow in front of the mirror is steady as opposed to the rear face of the mirror where the flow fluctuates the most. The turbulences at the rear face of the mirror create acoustic waves that travel rearward towards the side glass with a specific heading. This source term is associated to a dipole source (surface terms). The acoustic waves travelling towards the side glass are likely to be transmitted inside the vehicle through the side glass and to the driver's ear as illustrated in Figure 3 on the right.

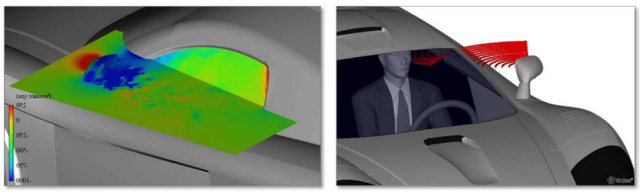

Figure 3. Fluctuating surface pressure on side mirror rear face (left) and acoustic waves propagating from side mirror to the driver's ear (right)

Pressure Fluctuation on A-Pillar

The same principle applies for the acoustic waves generated by turbulence in the vicinity of the A-Pillar. The acoustic waves travel to the side glass and are likely to be transmitted inside the vehicle to the driver's ear Figure 4.

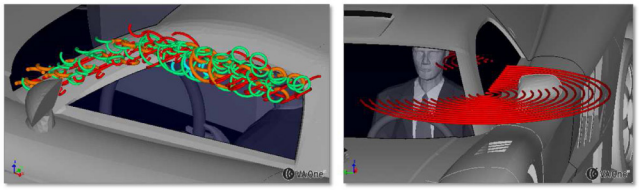

Figure 4. Fluctuating surface pressure on A-Pillar (left) and acoustic waves propagating from A-Pillar to driver's ear (right)

Acoustic Sources within Eddies

Eddies within the turbulent flow can also generate noise and therefore constitute acoustic sources. These sources act as quadrupole acoustic sources and are referred to as volume source terms. These acoustic sources are at close proximity to the side glass. At automobile speeds, these source terms are considered negligible (Figure 5).

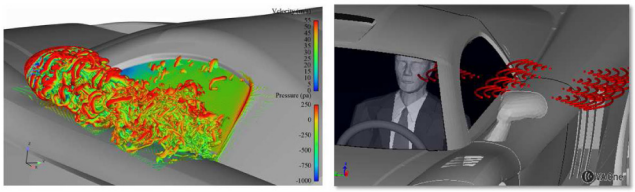

Figure 5. Turbulent flow behind side mirror (left) and acoustic waves propagating from within turbulent flow to the driver's ear (right)

Pressure Fluctuation on Side Glass - Outward Effect

Pressure fluctuations on the side glass also generate acoustic waves that propagate away from side glass. These waves can interfere with incoming acoustic waves from A-Pillar and mirror. It is believed to have a negligible impact on driver's ear SPL (Figure 6).

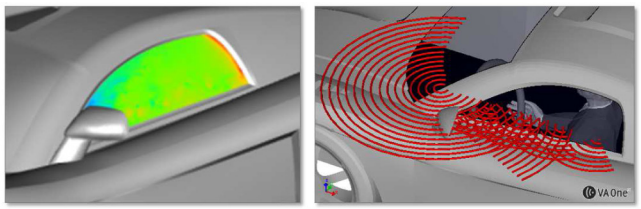

Figure 6. Fluctuating surface pressure on side glass (left) and acoustic waves travelling from side glass away from vehicle. The acoustic waves intefere with acoustic waves coming from side mirror and A-Pillar (right).

Overview of Available Approaches

Several methods of representing the wind noise sources have been investigated over the past 10 years in the automotive industry. Empirical methods have shown their merits and limitations especially when the geometry of the structure changes significantly compared to previous computations [1,2,3,4]. A more predictive approach, based on the ability of coupling time domain turbulent flow data to a vibro-acoustics model has opened new possibilities. The computation process is illustrated in Figure 7.

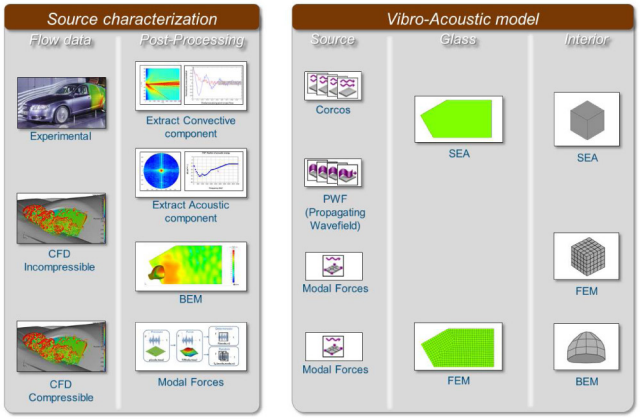

Figure 7. Illustration of source characterization (left) and vibro-acoustic modelling (right) approaches discussed in this paper

The left side of Figure 7 shows the source characterization topics that will be covered in the paper and the right side the vibro-acoustics methods that can be combined to compute the interior SPL. In this paper, the combination of the aero-acoustic (CAA) sources and a vibro-acoustic (VA) model is called an aero-vibro-acoustic (AVA) model.

Turbulent Flow Data

The turbulent flow can be represented by measurement of the fluctuating surface pressure on the side glass. In theory, these nodal time domain pressures include the convective and the acoustic component. Care must be taken to ensure both components are well sampled and represented in the data. Typically, surface pressure measurement points should be close enough to sample the short convective wavelengths at higher frequency. The microphones should be small enough to avoid “microphone size effect” at higher frequency. This subject is out of scope of this paper and more information can be found here [3,5,6]. Turbulent flow can also be represented using CFD compressible simulation which includes both convective and acoustic components. If, on the other hand, results of an incompressible CFD simulation are available then only the convective part will be represented by the CFD data since the fluid cannot transport the acoustic waves through compression and decompression of the fluid. In this case, the acoustic component can be computed using standard aero-acoustic analogies.

Post-Processing

Before discussing the fluctuating surface pressures post-processing approaches, it is useful to first investigate how different loads are transmitted through a typical side glass. In particular, it is often found that the glass acts as a spatial filter and preferentially transmits certain wavenumbers found in the fluctuating surface pressure data [7,8,9]. The spatial filtering of different exterior fluctuating surface pressures can be demonstrated using a simple numerical example. Figure 8 shows three glass panels of dimension 1 m × 1 m × 3.5 mm. Each has a constant structural damping loss factor of 6% and is placed in contact with a 1 m^3 acoustic cavity.

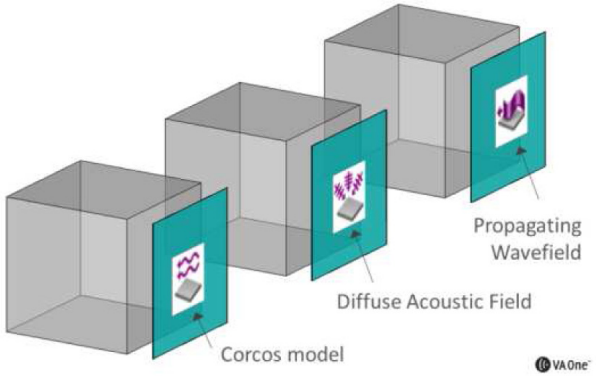

Figure 8. Glass panel of dimension 1 m^2 and thickness 3.5 mm in contact with a 1 m^3 acoustic cavity and excited by i) TBL (Turbulent Boundary Layer : Corcos model with a 40 m/s mean flow), ii) DAF (Diffuse Acoustic Field) and iii) PWF (Propagating Wave Field with directivity representing wave travelling from mirror).

A Turbulent Boundary Layer (TBL) based on Corcos model with a 40 m/s free stream velocity is applied to the first panel. A Diffuse Acoustic Field (DAF) representing waves having the same probability of impinging on the glass from any direction is applied to the second panel. Finally, a Propagating Wave Field (PWF) representing waves travelling with a specific heading as illustrated in Figure 9 is exciting the third panel. An angle φ equal to 70° is used since it is close to the one found between a mirror rear face and a side glass normal vector.

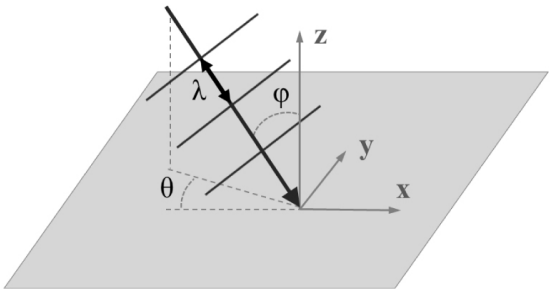

Figure 9. Propagating Wave Field incident angles description

The magnitude of the exterior fluctuating surface pressure of each load has been normalized to have unit amplitude. An SEA model is then used to predict the interior sound pressure levels of each cavity [10]. It can be seen in Figure 10 that even though the loads have the same exterior fluctuating surface pressure amplitude, the interior sound pressure level due to the Turbulent Boundary Layer is approximately 30dB lower than that due to the DAF and 10 to 30 dB lower compared to the PWF due to the different spatial correlation characteristics of each load.

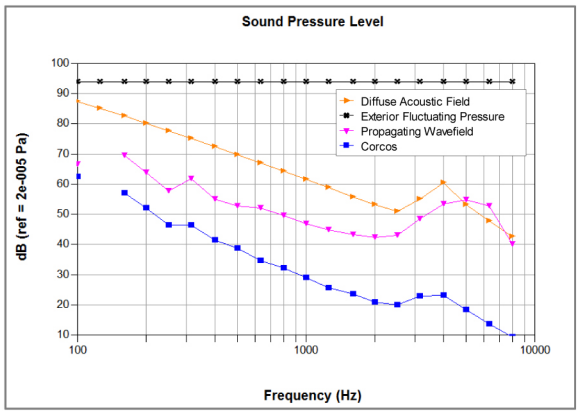

Figure 10. Sound Pressure Level inside cavities for three different loading. Note that the Turbulent Corcos load yield approximately 30 dB lower SPL inside the cavity, and 10 to 30 dB compared to the PWF due to the different spatial correlation characteristics of each load.

The reason for the difference in interior SPL is due to differences in the "spatial correlation" of the loads. The cross-spectra S_{pp} between two locations in a spatially homogenous fluctuating surface pressure can be written as

$$S_{pp}(x, x') = F(\omega)\, R(x, x', \omega) \tag{1}$$

where F is a function of frequency (that does not depend on location) and R represents a spatial correlation function. A diffuse acoustic field has a spatial correlation function R of the form [11]

$$R(x, x') = \sin(kr)/kr; \quad r = |x - x'| \tag{2}$$

where k is the acoustic wavenumber and r is the distance between two locations x and x' on the surface. A Turbulent Boundary Layer (modelled using a Corcos type model) has a spatial correlation function R of the form [12]

$$R(\Delta x, \Delta y) = \exp(-\alpha_x |\Delta x| - \alpha_y |\Delta y|)\exp(-ik_c \Delta x) \tag{3}$$

where Δx is the separation distance between two points in the flow direction, Δy is the separation distance in the cross flow direction, α_x and α_y are spatial correlation decay coefficients in the flow and cross-flow directions and k_c is the convection wavenumber.

For a side glass problem, the acoustic wavenumber is typically much lower than the convection wavenumber across much of the frequency range of interest (the DAF and PWF have a much longer spatial correlation length than the TBL source). The three different excitations therefore result in very different distributions of energy in wavenumber space, and this preferentially excites different structural mode shapes of the glass. The Diffuse Acoustic Field and Propagating Wave Field have a concentration of energy at low wavenumbers. Below glass coincidence, (peak in interior SPL around 4kHz is associated with the glass coincidence frequency) this typically excites the 'non-resonant' (mass controlled) modes of the glass. Since these modes are also efficient acoustic radiators, the mass controlled modes are typically the dominant transmission path below coincidence. Above coincidence, the resonant modes become the dominant transmission path but these modes are also well excited by the wavenumber content of a DAF or PWF. In contrast, a Turbulent Boundary Layer typically has a concentration of energy at the convective wavenumber of the flow and has much smaller concentrations of energy at the wavenumbers associated with the resonant and mass controlled modes of the panel. The net result is that a DAF or PWF is transmitted through the glass much more efficiently than a Turbulent Boundary Layer for the same RMS fluctuating surface pressure. In summary, in order to characterize an exterior fluctuating surface pressure and enable design changes that would best impact interior noise, it is necessary to be able to characterize not only the magnitude of the fluctuating surface pressure but also its wavenumber content.

Extract Convective Component

The convective component of a turbulent flow can be represented as a Corcos model. This empirical approach has been widely used in the past in the aerospace industry [9, 12, 13, 14, 15, 16] and has recently been applied with success in the train and automotive industry for wind noise application [6, 17, 18, 19, 20].

A fundamental hypothesis of a Corcos model is that the turbulent flow should exhibit a spatially homogenous fluctuating surface pressure character on a surface. It has been observed that on a side glass surface three main regions have been identified: the mirror wake, the A-Pillar vortex and a reattached region. These regions typically exhibit very different flow characteristics and can be modelled using several Corcos sources with parameters corresponding to each flow region. These various sources can be applied to a single SEA panel for example. One can decide to use an average set of Corcos parameters representing the side glass in its entirety. In this case, a single TBL source would be applied on the side glass SEA panel.

The extraction of the Corcos parameters such as the spatial correlation decay coefficients in both flow and cross-flow direction and the convection wavenumber from the turbulent flow data is illustrated in Figure 11 and implemented in [10]. Step 1 shows the spatial distribution of the auto-spectra of pressure. Step 2 shows the normalized spatial correlation in flow (blue) and in cross-flow (red) direction with respect to nodal distance extracted from the turbulent flow data. The full cross-spectral matrix is calculated for a (dense) grid of points across the surface region of interest. A spatial averaging is performed by using bins in which nodes are grouped as illustrated in step 3. This surface region is divided into a coarser orthogonal grid and a reduced cross-spectral matrix is obtained by averaging the auto-spectra and cross-spectra within each cell of the coarse grid. Spatial correlation functions R_{pp} are then obtained by averaging overall all pairs of cells with the same separation distance in the flow and cross-flow

directions. In step 4, the log of the resulting cross-correlation function is used to extract the spatial correlation decay coefficient in flow and cross-flow direction. Finally, step 5 shows how the phase of the resulting cross-correlation function is used to extract the convective wavenumber.

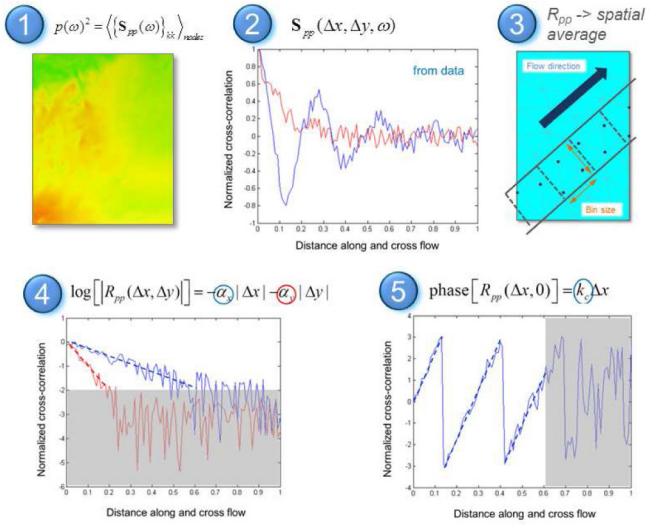

Figure 11. Extracting convective component from turbulent flow.

Extract Acoustic Component

In the previous section, the spatial correlation function was presented with respect to distance between two points. Using a 1D wavenumber transform it is possible to visualize the spatial correlation function in terms of wavenumber content vs frequency (Figure 12).

P(X,t) -> P(X,ω)) -> Rpp(Δx,ω) -> Rpp(kx,ω)
P(X,t) -> P(X,ω)) -> Rpp(Δy,ω) -> Rpp(ky,ω)

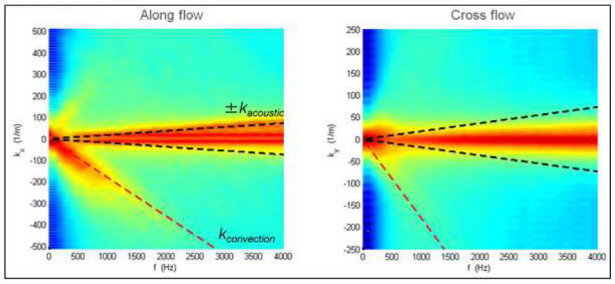

Figure 12. 1D wave number transform of a turbulent flow surface pressure.

The wavenumber content in the flow and cross-flow direction can also be obtained by calculating the 2D wavenumber transform of the spatial correlation functions obtained in the previous section (at each frequency of interest). The magnitude of the 2D wavenumber transforms for two frequencies are plotted in Figure 13 (the scale of the contour plot is approximately 30 dB). The acoustic circle is shown in white in the figure, and the convection wavenumber for a 30 m/s flow is plotted as a straight line segment. It can be seen that at low frequencies, there are two distinct concentrations of energy in wavenumber space at the convective wavenumber and at acoustic wavenumbers. At higher frequencies, there is little evidence of any energy at the convective wavenumbers. This may be physical but it may also perhaps be an artefact of the CFD calculation.

P(**X**,t) -> P(**X**,ω)) -> $R_{pp}(\Delta x, \Delta y, \omega)$ -> $R_{pp}(kx, ky, \omega)$

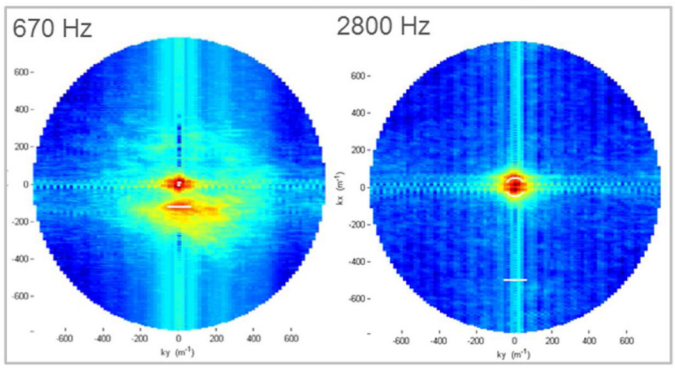

Figure 13. 2D wavenumber transform of a turbulent flow surface pressure

Comparing Figure 11 step 1, Figure 12 and Figure 13, it can be seen that a complex distribution of energy in the spatial domain becomes a much simpler distribution of energy in the wavenumber domain (1D and 2D). It is possible to fit an equivalent acoustic source (DAF or PWF) to the CFD data by integrating the energy in the acoustic circle in wavenumber space. The RMS pressure spectrum for the total fluctuating surface pressure field and its acoustic component (DAF) are shown in Figure 14. Below 350Hz there is less than one acoustic half wavelength across the dimension of the side glass and so there is not enough resolution in the wavenumber transform to provide a good estimate of the acoustic wavenumber content. However, for wind noise applications interest typically lies in higher frequency content and so this is not a significant constraint. It can be seen that the estimated amplitude of the acoustic component is 5-30dB less than the amplitude of the overall fluctuating surface pressure. However, since the glass is 30dB more sensitive to an acoustic component than to a convective component as previously shown the acoustic component can often be one of the dominant contributors to interior noise.

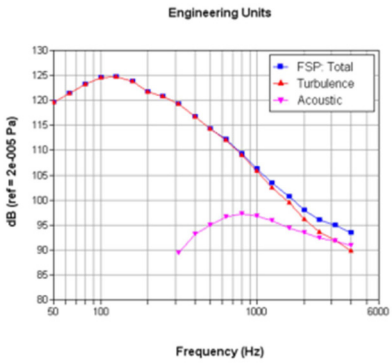

Figure 14. Turbulent flow total surface pressure (blue), convective part (red) and acoustic component (pink)

Using BEM to Propagate External Acoustics

The Navier-Stokes equations are notoriously difficult to solve numerically, and a wide range of approximate strategies has been developed (LES, RANS, etc) to do so. In particular it is

very difficult to solve for both turbulent flow and acoustic radiation at the same time, since turbulence is small scale and requires a very fine grid of computational mesh points and acoustic waves and sound radiation require a large spatial region to be modeled. Most CFD codes avoid this problem by assuming that the flow is incompressible which removes the acoustics [21]. This section discusses how the acoustics can be added to an incompressible CFD simulation.

For wind noise automotive application, this means using BEM to propagate acoustic waves generated from the fluctuating surface pressure locations such as mirror and A-Pillar surfaces towards the side glass (see Figure 15)

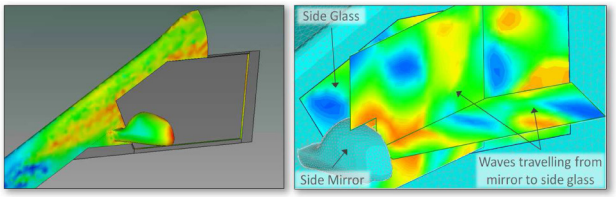

Figure 15. CFD fluctuating surface pressure imported on mirror and A-Pillar (left) applied as a boundary source term on a BEM model that propagates acoustic waves from mirror and A-Pillar to side glass

New derivation of the acoustic analogy based on Curle's integral version of the Lighthill equation for BEM allows the use of CFD incompressible analysis to model the turbulent flow. CFD pressure time history data are then directly imported into [10] which uses this CFD data as a source for a BEM fluid and computes acoustic propagation and scattering. The use of time domain surface pressure data translates into small file sizes and fast calculations. This method is also less sensitive to mesh projections than other formulations using volume terms. The only restriction is that the near fields from quadrupole source terms are neglected. The theory behind this method is strictly valid for flows with low Mach numbers (Ma<0.3) where surface terms dominate. In addition to exterior wind noise modelling, this approach can also be used to model flow induced duct noise such as automotive HVAC systems.

In summary, the Curle's approach is used to split the original set of volume sources into a set of surface sources (dipoles) and a set of remaining volume sources (quadrupoles). The quadrupole volume sources are then neglected; this means that only the hydrodynamic pressure on the surface is needed for the analysis. In contrast (for example) a volume code does not apply Curle's approach and retains the original set of volume sources, thus requiring full hydrodynamic flow information for the acoustic solution.

Modal Forces

When FEM is used to represent the side glass, one can directly use the time domain fluctuating surface pressure and convert them into modal forces. The process is illustrated in Figure 16. The time domain pressures are converted into forces and projected onto the modes of the side glass. The full time domain modal force signal is then either used in its entirety as a single window and used in the AVA model as a deterministic excitation or the time signal is post-processed and averaged using overlapping segments to generate a random source.

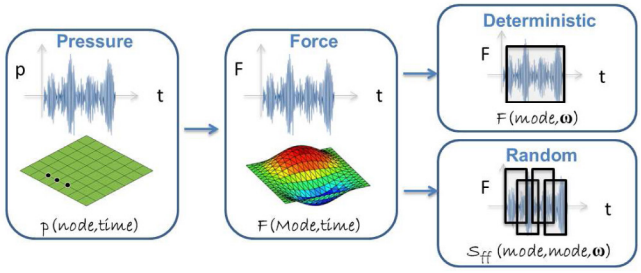

Figure 16. Using modal forces to represent forcing function from turbulent flow.

Description of the Vibro-Acoustic (VA) Model

The vibro-acoustic model is composed of a source, a transfer path (the side glass) and a receiver. This VA model offers the possibility to mix and match different VA methods depending on user requirements in terms of accuracy, computation time, time needed to build a model and source data availability.

Wind Noise Source Representation

As previously described, a Corcos model can be used to represent the convective source term of a turbulent flow in a VA model. This source can be applied to a SEA or FEM panel. The Corcos parameters can be either extracted from measured data or from a CFD computation.

The acoustic component of a turbulent flow can be represented by either a DAF or a PWF. These sources can be applied to a SEA or FEM panel. The amplitude of the pressure field can be either computed from a 2D wavenumber transform or a BEM computation where incompressible CFD data is used as boundary condition.

Finally, modal forces can be used to project the fluctuating surface pressure onto the modes of a FEM panel. This approach can be used with data that contains both convective and acoustic component or it can be used with data containing only a single component. The latter permits the calculation of the contribution of each component separately.

Modelling the Side Glass

The side glass can be either tempered or laminated. Several modelling approaches can be used to best represent the behaviour of the glass and this is out of the scope of the present paper. Note that a side glass has typically a few hundred modes up to 5kHz and do not represent a large computation expense compared to the interior volume of the vehicle. Furthermore, the use of FEM allows the designer to test different boundary conditions and complex lamination to find the best possible design.

One can also use a SEA glass which permits a fast computation and a reliable prediction of the overall behaviour of the glass especially at higher frequencies where the glass coincidence frequency makes the glass acoustically transparent. Laminated glass can also be model accurately using SEA and a 1D FEM model implemented in the general laminate module in [10].

Modelling Vehicle Interior

The interior of a vehicle can be modelled as a SEA, a FEM or BEM fluid domain. The number of modes in the interior volume can be as high as 10 000 below 3 kHz (see Table 1). SEA models used to compute the response of such a volume can solve in a few minutes, where BEM might take a few days and FEM would be impractical to do in modal response. The advantage of a deterministic method such as BEM is that the response can be computed at specific microphone locations. SEA will provide the average SPL in a location such as the driver headspace. An important aspect of the interior volume is the localized absorption which will affect the way acoustic waves will travel in the volume.

Table 1. Mode count for SAE body interior cavity

Frequency (Hz)	Mode count
125	5
250	23
500	123
1000	770
2000	5340
4000	39246
8000	301012

Computing the wind noise contribution to total SPL at driver's ear can be quite simple if one only accounts for the transfer through the side glass. There is no need to create a full vehicle VA model, the interior fluid cavity with the right surface absorption is sufficient. Nonetheless, the final objective is usually to include the wind noise sources into a full vehicle model and make design changes that will either improve passengers experience or reduce cost while maintaining vibro-acoustic performance of the vehicle.

Approach Selection based on Design Process Phase

The adequate approach to select depends on many factors:

- Available turbulent flow data
- Available computation resources
- Available resource/time for model building
- Available time for computation
- Design process stage
- Required accuracy
- Absolute vs relative interior noise levels

The following sections illustrate several possible approaches and discuss the advantages and inconveniences of their use. Several variants are not covered by this paper and will have to be addressed at a later time. The selected approaches are organized based on the turbulent flow data availability and side glass modelling method.

Experimental Wind Tunnel Flow Data Available

SEA Side Glass Approach

When experimental wind tunnel test data are available, several approaches can be selected to predict interior vehicle SPL. Figure 17 shows the case where the convective and acoustic components are extracted and a SEA side glass is used in conjunction with either a SEA or a FEM interior fluid. This approach has the advantage of being very fast to compute and setup. Once both components of turbulent flow are extracted, the wind noise contribution to interior SPL is computed in minutes. The model setup is also fast, using either a single cavity model or a full vehicle coarse SEA model for target setting of different sub-assembly or a detailed full vehicle SEA model if one is available. Predictions are averaged over a volume around the passenger's head unless a FEM cavity is used, then a specific microphone location can be predicted but this only at frequencies below coincidence frequency as mentioned earlier.

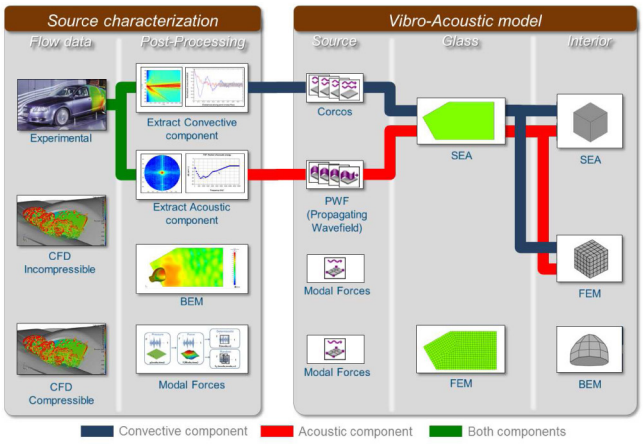

Figure 17. Using experimental wind tunnel data and a SEA or FE/SEA model to predict interior wind noise

Drawbacks to this approach are that a clay model or prototype is needed to perform wind tunnel test. To properly extract the convective component, the measurement locations have to be chosen adequately [6]. Finally, frequency domain of validity of the extracted convective component might be limited and well below the coincidence frequency of the side glass due to the number of modes in the FEM interior volume.

FEM Side Glass Approach

Figure 18 shows the case where the modal forces are used to represent the turbulent flow and a FEM side glass is used in conjunction with a BEM, a FEM or SEA interior fluid. This approach has the advantage of being very accurate since the source data is taken as is, converted into modal forces, applied on a FEM panel and a deterministic interior fluid can be used. The model setup is simple and can be completed within a few hours. A SEA interior fluid cavity can also be used to increase frequency range of computation to higher frequencies than the glass coincidence and therefore reduce computation time.

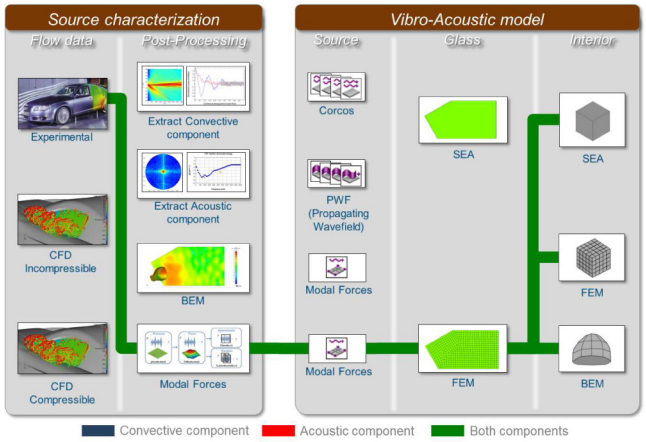

Figure 18. Using experimental wind tunnel data and a BEM or FEM or FE/SEA model to predict interior wind noise

Drawbacks to this approach are that a clay model or prototype is needed to perform wind tunnel test. To properly capture the convective component, the measurement locations have to be chosen adequately [6]. The contribution from the convective and acoustic component cannot be separately computed. Finally, frequency domain of validity of the convective component might be limited and well below the coincidence frequency of the side glass because of shorter correlation length as the frequency increases.

CFD Incompressible Flow Data Available

SEA Side Glass Approach

When CFD incompressible turbulent flow data are available, several approaches can be selected to predict interior vehicle SPL. Figure 19 shows the case where the convective component is extracted from the data to find the Corcos parameters. It also shows that the acoustic component is evaluated by means of a BEM model propagating the acoustic waves from the fluctuating surface pressure locations towards the side glass. Finally, a SEA side glass is used in conjunction with either a SEA or a FEM interior fluid. This approach has the advantage of being fast to compute. Once both component of turbulent flow are extracted, the wind noise contribution to interior SPL is computed in minutes. The model setup is also fast, using either a single cavity model or a full vehicle coarse SEA model for target setting of different sub-assembly or a detailed full vehicle SEA model if one is available. Interior SPL predictions are averaged over a volume around the passenger's head unless a FEM cavity is used, then a specific microphone location can be predicted but this only at frequencies below coincidence frequency as mentioned earlier. Finally, using CFD incompressible removes the burden of having to transport the acoustic waves inside the CFD simulation. This simplifies the otherwise complex CFD model setup needed for compressible simulation.

Drawbacks to this approach are that a CFD incompressible flow data is needed which can take several days to run. In this approach, an additional exterior BEM model is needed to characterize the acoustic component. The BEM computation can take several days.

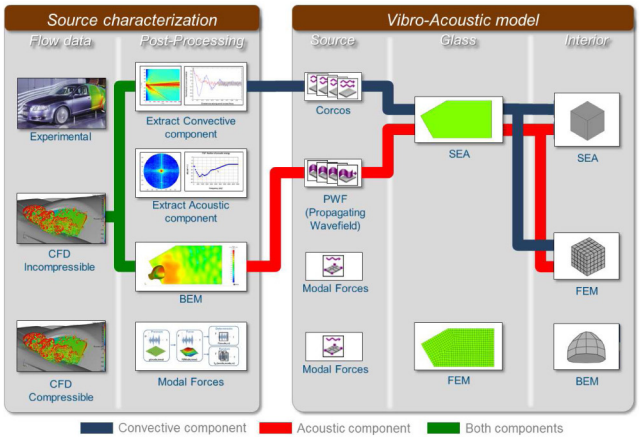

Figure 19. Using CFD incompressible data and a SEA or FE/SEA model to predict interior wind noise

FEM Side Glass Approach

Figure 20 shows the case where the modal forces are used to represent the turbulent flow and a FEM side glass is used in conjunction with a BEM, a FEM or SEA interior fluid. This approach has the advantage of being accurate since the convective source data is taken as is, converted into modal forces, applied on a FEM panel and a deterministic interior fluid can be used. The acoustic component uses the Curle's integral formulation of Lighthill, therefore an approximation is done on this acoustic component. The contribution to interior noise of the convective and acoustic component is possible with this approach. A SEA interior fluid cavity can also be used to increase frequency range of computation to higher frequencies than the glass coincidence and reduce computation time. The model setup is simple and can be completed within a few hours.

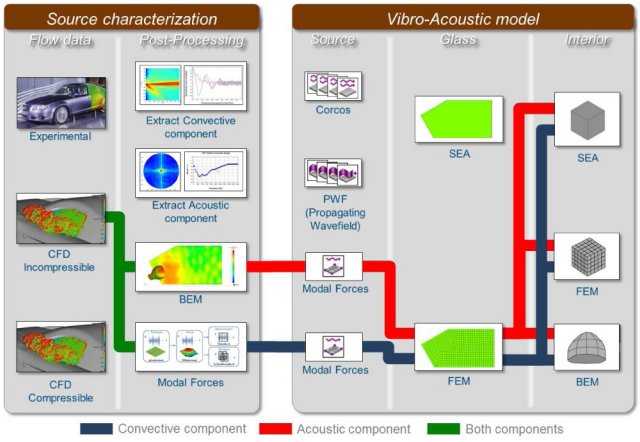

Figure 20. Using CFD incompressible data and a BEM or FEM or FE/SEA model to predict interior wind noise

Drawbacks to this approach are that a CFD incompressible flow data is needed which can take several days to run. In this approach, an additional exterior BEM model is needed to characterize the acoustic component. The BEM computation can take several days.

CFD Compressible Flow Data Available

SEA Side Glass Approach

When CFD compressible turbulent flow data are available, several approaches can be selected to predict interior vehicle SPL. Figure 21 shows the case where the convective component is extracted from the data to find the Corcos parameters. It also shows that the acoustic component can be evaluated using the 2D wavenumber transform described earlier. Finally, a SEA side glass is used in conjunction with either a SEA or a FEM interior fluid. This approach has the advantage of being fast to compute. Once both component of turbulent flow are extracted, the wind noise contribution to interior SPL is computed in minutes. The model setup is also fast, using either a single cavity model or a full vehicle coarse SEA model for target setting of different sub-assembly or a detailed full vehicle SEA model if one is available. Interior SPL predictions are averaged over a volume around the passenger's head unless a FEM cavity is used, then a specific microphone location can be predicted but this only at frequencies below coincidence frequency as mentioned earlier.

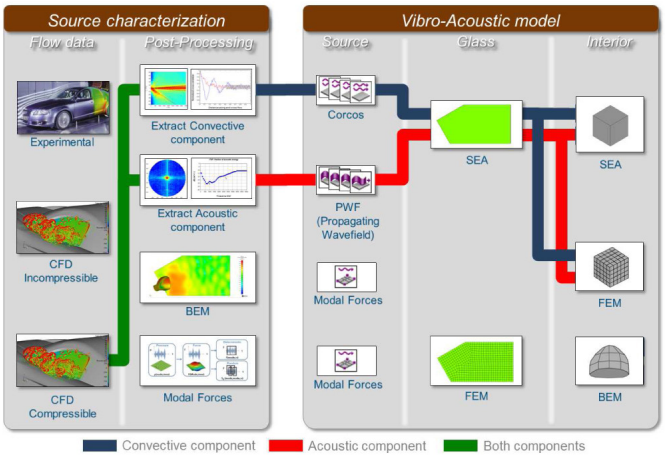

Figure 21. Using CFD compressible data and a SEA or FE/SEA model to predict interior wind noise

Drawbacks to this approach are that a CFD compressible flow data is needed which can take several days to run. The complex CFD model setup needed for compressible simulation should not be neglected; getting the acoustic waves to properly travel in the CFD fluid is not an easy task.

FEM Side Glass Approach

Figure 22 shows the case where the modal forces are used to represent the turbulent flow and a FEM side glass is used in conjunction with a BEM, a FEM or SEA interior fluid. This approach has the advantage of being accurate, provided that the source data is accurate, since the CFD source data is taken as is, converted into modal forces, applied on a FEM panel and a deterministic interior fluid can be used. A SEA interior fluid cavity can also be used to increase frequency range of computation to higher frequencies than the glass coincidence and therefore reduce computation time. The model setup is simple and can be completed in a few hours.

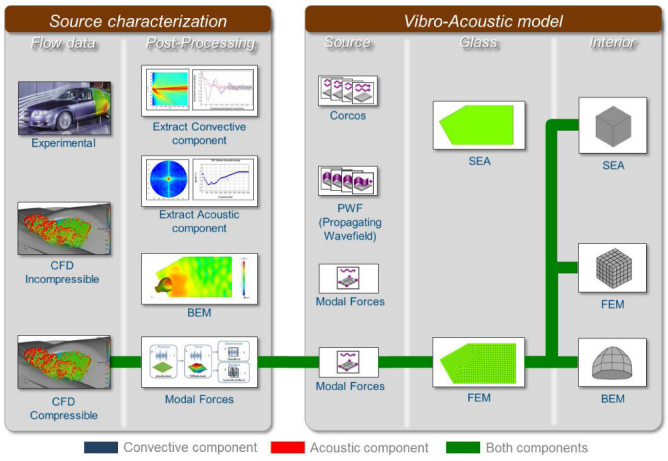

Figure 22. Using CFD compressible data and a BEM or FEM or FE/SEA model to predict interior wind noise

Drawbacks to this approach are that a CFD compressible flow data is needed which can take several days to run. The contribution from the convective and acoustic component cannot be separately computed. This computation can take several days to run if BEM or FEM is used to model the vehicle interior.

The Right Model at the Right Time

Design decisions are based on information and simulation models available at a certain time. These vary greatly if one is at an early stage of product design or at a validation phase. Figure 23 illustrates a product design process and where the approaches described in previous sections can be used. At an early stage, the side glass SEA based approaches are to be favoured since the computation time is short and trends can be rapidly identified for a specific design (see approaches 1,2,3 in Figure 23). If actual turbulent flow source data is not available yet, the convective and acoustic parameters can always be replaced with the ones from a predecessor vehicle and an early stage computation can be readily available in minutes. The experimental flow source is placed further down the design process since the availability of a prototype comes only at a later stage and only a limited set of measurement can be done on a clay model. Later in the design process, more accurate and computationally demanding approaches can be used such as 4,5 and 6 in Figure 23. These are based on side glass FEM modelling and require much longer run time providing an answer several weeks after the start of the CFD and AVA model building.

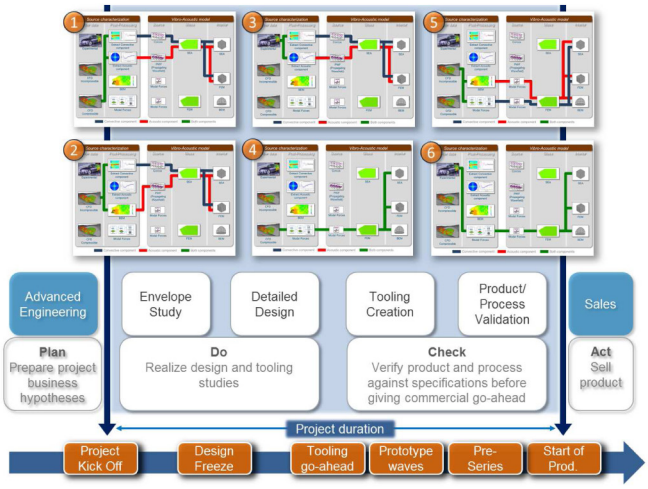

Figure 23. Various approaches for various design process stages. SEA modelling preferred at early stages and deterministic combined with measurements for final verification stages.

It is difficult to categorize the approaches above since the SEA based approaches could also be used for design optimization of A-Pillar and mirror shapes. Once a few design iterations have been pre-selected using CFD-SEA, one could validate the best solution with a more accurate approach before test data is even available. The approaches described here provide flexibility to the user and allow him to select the methods best suited to efficiently answer a question on design change.

Vibro-Acoustic (VA) Validation

In order to experimentally validate some of these aero-vibro-acoustic approaches to ensure an accurate prediction of interior SPL contribution from wind noise, one must first validate the vibro-acoustic models with ideal sources. The objective is to confirm that the vibro-acoustic model can properly represent the behaviour of the vehicle under controlled acoustic excitation before starting to use turbulent flow source data. This section describes the vibro-acoustic validation performed in a semi-anechoic room. The last section of this paper presents the validation of aero-vibro-acoustic models using wind tunnel measurements. These two sections have been done in collaboration with the CAA German Working Group (Audi, Daimler, Porsche and VW) and are based on test campaigns published in 2012 [5].

Description of VA Validation Cases

Description of the SAE Body

The SAE body is a generic vehicle model based on the SAE Type 4 (fullback). It is built out of stiff foam and is designed to be used in the current wind noise study which includes acoustic measurements in the cabin, leading to the following requirements of the physical model:

- The noise transmission into the cabin interior needed to be reduced to one relevant acoustic transfer path through the left front side window. This reduces the problem encountered as much as possible when comparing experimental and simulation results.
- The flow over the A-pillar and rear view mirror region, which causes the aero-acoustic excitation of the side window, should be similar to a real car
- Variability of the aero-acoustic excitation by changing components as well as the possibility to modify the acoustic transfer properties of the side window
- A quick set-up of modifications and variants to save time during the wind-tunnel measurement

For more information on the SAE body, please refer to [5]. Figure 24 and Figure 25 show the SAE body geometry, the side mirror, side glass and a view of the thickness of the walls.

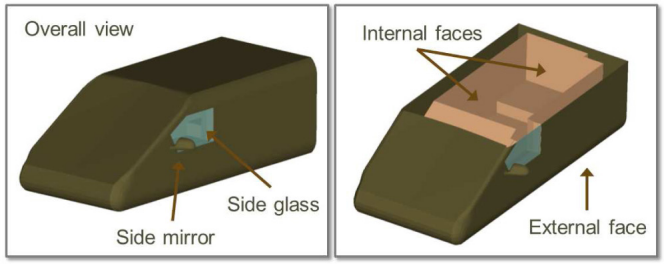

Figure 24. SAE body description: Note the generic shape, the side mirror, side glass, outer and inner faces.

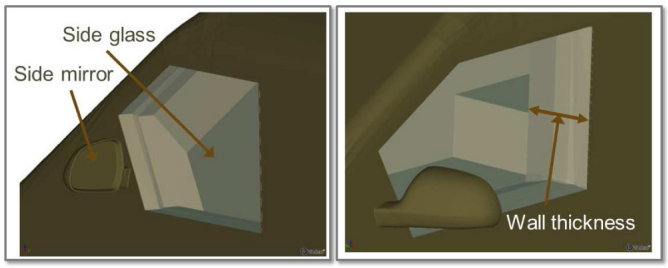

Figure 25. SAE body is quite thick, side glass is mounted flush to outer face.

Noise Reduction (NR) Consideration

A noise reduction test was performed to assess the ability of the SAE body walls to block the transfer of acoustic energy and compare the NR wall results with the side glass data. NR is the ratio of the average acoustic pressure inside the SAE body and the average SPL from a microphone scan over different regions. To perform this test, an omnisource from B&K was placed inside the SAE body (see Figure 26). A microphone measured SPL inside the source during testing.

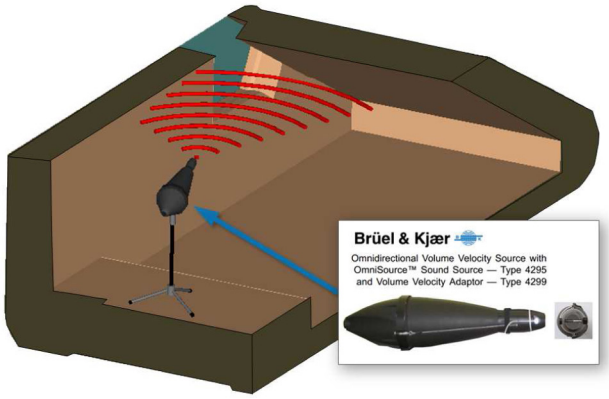

Figure 26. An omnisource is located inside the SAE body to fill interior volume with a strong acoustic field

A set of 5 microphones were placed inside the SAE body to measure the SPL at each location and the average interior SPL (Figure 27).

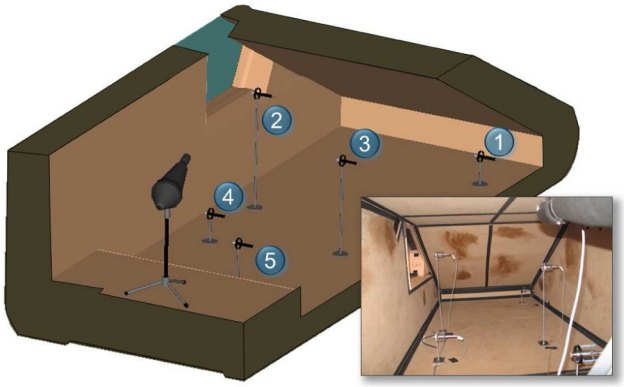

Figure 27. 5 microphones are located inside SAE body to monitor interior sound field.

A set of seven patches were defined to assess NR of different walls. Figure 28 shows the patches where exterior SPL was measured close to the surface of each wall.

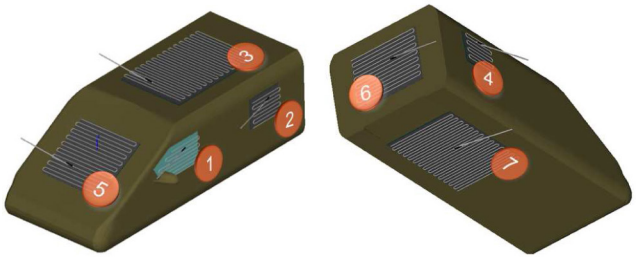

Figure 28. Noise reduction (NR) patches where average SPL is measured.

Figure 29 shows the actual SAE body in the semi-anechoic room where measurements were performed (left) and how the scanning was done (right).

The results shown in Figure 30 indicate that below 400 Hz, the wall NRs are comparable to the side glass NR. This suggests that care must be taken when interpreting the results in this frequency domain since energy might actually be transferred not only through the side glass but also through the walls. At higher frequencies, only the rear panel exhibit a low NR compared to the glass. This is considered less of a problem since the rear panel is far away from the side glass.

Figure 29. Noise Reduction (NR) measurements performed on several patches around the SAE body.

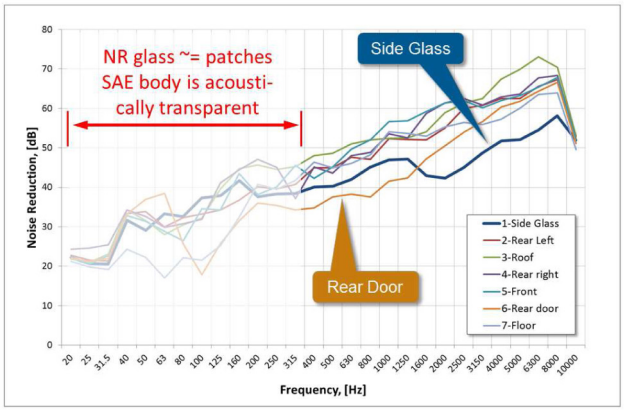

Figure 30. Noise Reduction (NR) results. Starting at 400 Hz, the SAE body patches offer a NR that is higher than the side glass. Below 400 Hz, patches are acoustically as transparent as the side glass.

Test results show that NR SAE body roof, wall and floor are on average 10 dB higher than the side glass at frequency higher than 400 Hz. Region of interest around glass resonance frequency (~3 kHz) show higher NR.

VA Simulation Models

Several VA simulation models were built to assess their performance in accuracy and computation time. Figure 31 shows the three models presented in this article.

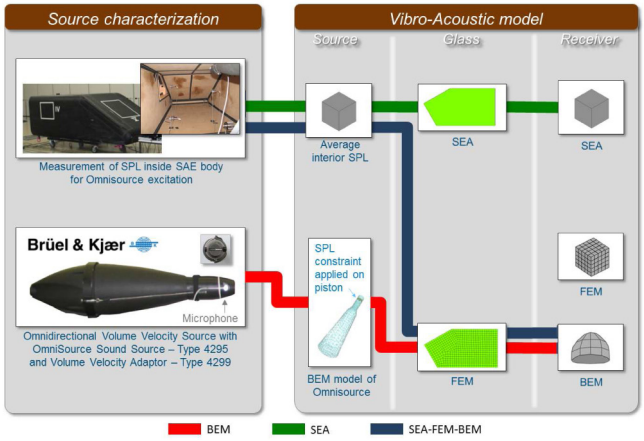

Figure 31. Validation of the vibro-acoustic model is done for different modelling methods representing different parts of the system taking advantage of the strength of each method in terms of speed and accuracy

The BEM model (red in Figure 31) consists of a BEM interior fluid where a BEM model of the omnisource has been built. The source model is based on [22,23]. The measured SPL inside the omnisource is used as a constraint on a flat surface inside the BEM omnisource model. The side glass is represented in FEM and the external fluid is also modelled with BEM.

The SEA model (green in Figure 31) uses the average SPL measured inside the SAE body as a constraint on an SEA interior cavity. The side glass is also modelled using SEA and the external sound field is represented using a semi-infinite fluid which represents an anechoic termination.

The SEA-FEM-BEM model (blue in Figure 31) uses the average SPL measured inside the SAE body as a constraint on an SEA interior cavity. The side glass is represented in FEM and the external fluid is modelled with BEM. The formulation behind this fully coupled method called “FE/SEA Coupled” can be found in [24,25].

Omnisource Inside SAE Body

For VA validation, the omnisource was placed inside the SAE body and prediction were compared with measurement for i) SPL at interior microphone location, ii) side glass acoustic power radiated and iii) external SPL at different angles from side glass.

Interior SPL at Microphone Locations

Figure 32 shows comparison of measurements with BEM predictions of SPL at microphones locations and the average levels. At lower frequency, difference between simulation and test can be explained by the fact that in the simulation, the SAE body walls are considered rigid. In reality, there is energy dissipated within the walls and energy transmitted outside though every walls. It also shows at higher frequencies that SPL can be predicted with reasonable accuracy suggesting that the Omnisource BEM model is acceptable.

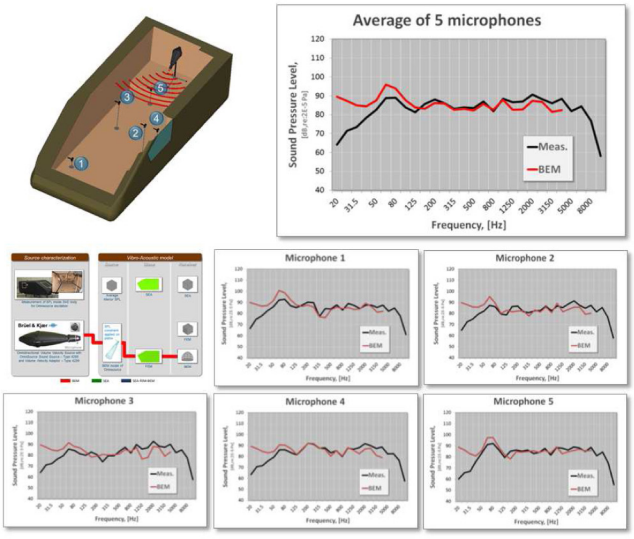

Figure 32. Predicting SPL inside SAE body generated by an omnisource inside

Acoustic Sound Power Radiated by Side Glass

Figure 33 shows that the acoustic power radiated by the side glass is predicted with high accuracy using either BEM or a pure SEA approach. For SEA, prediction has been done up to 10 kHz in a few seconds.

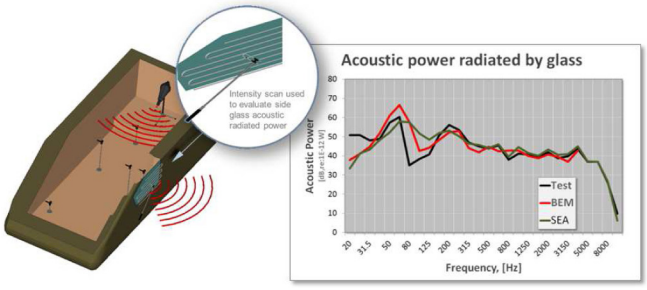

Figure 33. Radiated acoustic power from side glass. Both SEA and BEM are accurate and SEA is computed up to 10 kHz in seconds

External SPL at Various Angles

The objective of this case is mainly to see if the VA models can predict the interaction between internal and external acoustic waves when they travel through the side glass. Figure 34 shows correlation results between measurements and BEM and SEA-FEM-BEM. Below 400 Hz, the acoustic energy travelling through the SAE body walls is clearly visible and explains why the measurements over-predict the SPL at microphone locations. Over 400 Hz, correlation is acceptable and show that the SEA-FEM-BEM computation yield accurate results for 1/10th of the computation time of BEM.

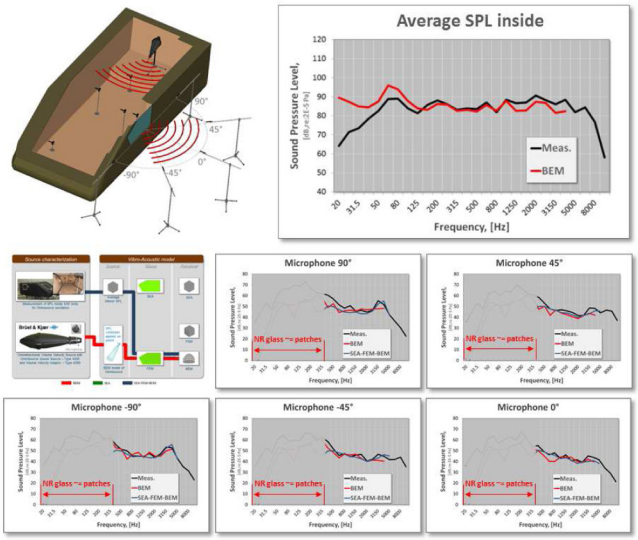

Figure 34. Predicting SPL at different angles from side glass for an omnisource located inside the SAE body. Note that below 400 Hz, the measurements show higher SPL levels since SAE body walls let acoustic energy travel outside. Walls are considered rigid in BEM simulation.

Omnisource Outside SAE Body

Finally, the omnisource was placed outside the SAE body and predictions and measurements were compared for SPL inside the SAE body. Figure 35 shows results for the case where the omnisource is placed at 1 meter and 0° from the side glass

normal vector. Correlation levels are very high and one can note that even below 400 Hz, the measured and predicted levels are quite similar. This can be explained by the fact that any acoustic energy entering the SAE body interior through the walls from the source side can easily exit from any other sides since the walls are acoustically transparent compared with the side glass at these low frequencies.

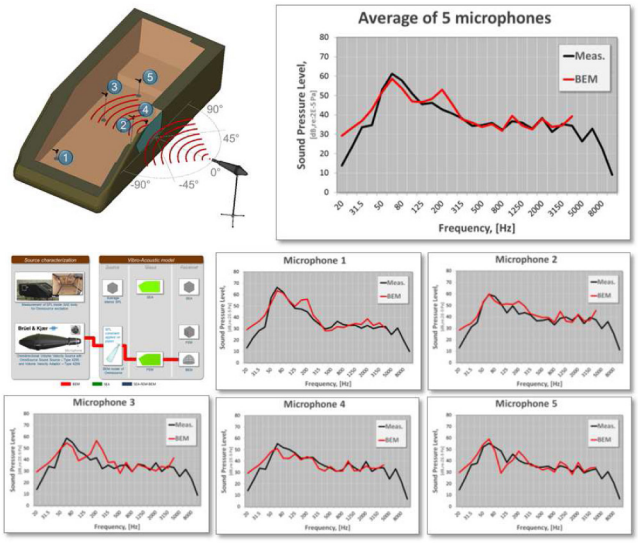

Figure 35. Predicting SPL inside SAE body for an omnisource outside at 0°. Low frequency correlation is acceptable in this case since any energy getting inside SAE body through the walls can get out on the opposite side of the SAE body.

Figure 36 shows the same level of correlation for the case where source is placed at 1 meter and −45° from the side glass.

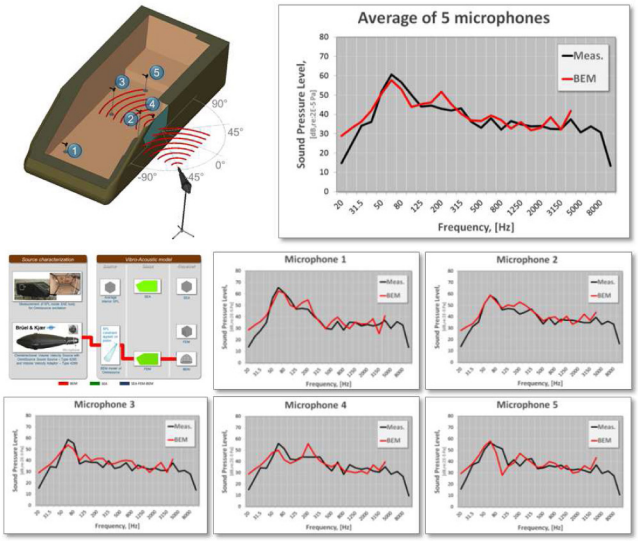

Figure 36. Predicting SPL inside SAE body for an omnisource outside at −45°.

Figure 37 shows the same level of correlation for the case where source is placed at 1 meter and −90° from the side glass. Note that the character of the response is quite different from one location of the source to the other and that the BEM model can properly track the changes in response. This is quite comforting since this is a configuration very similar to the real life case where the acoustic waves are believed to come from the front of the side glass where the mirror and A-Pillar are located.

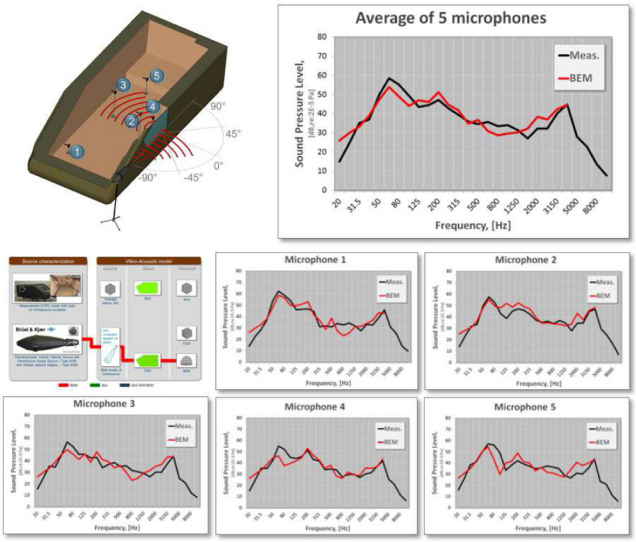

Figure 37. Predicting SPL inside SAE body for an omnisource outside at −90°.

Validation of Aero-Vibro-Acoustic Models

Experimental Setup

The measurements are described in details in [5]. Figure 38 shows on the left the SAE body in the wind tunnel for the configuration where the vibrations on side glass and SPL inside the SAE body are measured. The right side of the figure shows the surface mounted microphones used to measure the fluctuating surface pressure at the location of the side glass.

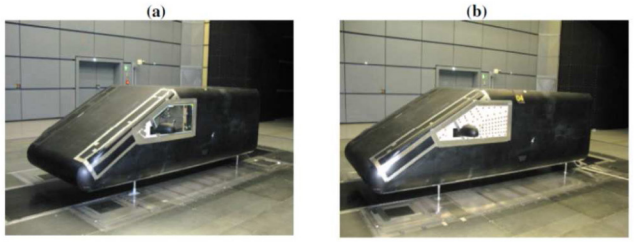

Figure 38. Wind-tunnel test: (a) glass module, (b) sensor module

Figure 39 shows in more details the microphones used to measure the fluctuating surface pressure.

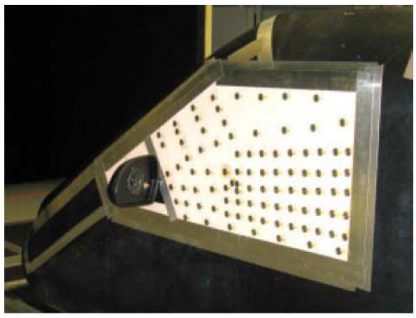

Figure 39. Surface microphones over side glass area.

CFD Data

The CFD data used for the prediction of wind noise inside the SAE body is the following:

- StarCCM+ Version 6.06.017
- Half model of an SAE body, a very basic car shape on struts, with a rear mirror (and a side glass with 10mm downset, i.e. side glass not flush-mounted)
- Model size: 45 up to 46 million fluid cells (dependent on configuration with/without 10mm Downset)
- Compressible Detached Eddy Simulation (DES) based on Spalart-Allmaras (S-A)
- Δt CFD = 2E-05s
- First 0.1s of simulated physical time has been cut away: spurious transition phenomena when starting a transient computation based on steady state results

The pressure time history data was imported into the commercial vibro-acoustics software in [10].

AVA Models

Figure 40 shows the SEA model containing the convective (Corcos) and acoustic (PWF) source, along with the SEA panel, area junction and the SEA cavity. Source levels and parameters were extracted from the CFD data based on earlier sections. This model runs in seconds.

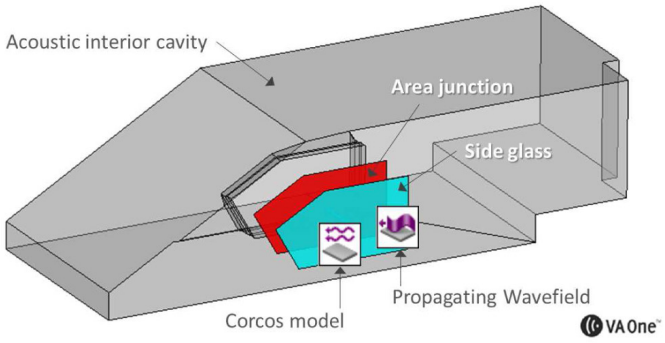

Figure 40. SEA model including interior cavity, side glass panel, area junction and wind noise sources.

Figure 41 shows the BEM model. For clarity, a mesh with coarse element size was used to generate the image but of course a smaller element size is needed to compute to higher frequencies. The BEM mesh allows for the prediction of SPL at any location inside and outside the SAE body. Five virtual microphones were located at the same location as in the measurements. A time domain FSP (Fluctuating Surface Pressure) source is connected to the side glass to allow the CFD data to be read in the model. CFD pressure data imported can be visualized as a contour plot in the current frequency domain set in the BEM model.

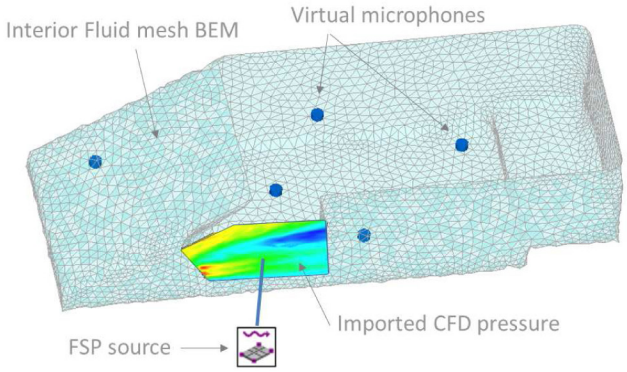

Figure 41. BEM model including FEM side glass, BEM interior fluid and a wind noise (FSP) source.

Preliminary AVA Validation Results

The following results are only presented as illustration of type of correlation that has been achieved so far on a few configurations. It does not constitute a recommendation of preferred approaches but merely an indication of what are the next results that will be published at a later time.

Figure 42 shows the average SPL inside SAE body generated by a 140 km/h wind predicted using the SEA model. The contributions from convective and acoustic component are also shown and were computed from 1D and 2D wavenumber transforms. At low frequency, the noise entering the SAE body from all sides contribute to an increase in measured SPL that is not reflected in the predictions since the SAE body walls are considered rigid in the simulation. The measurement should be compared with the blue line which is the sum of the convective and acoustic component. Computations to higher frequencies are underway.

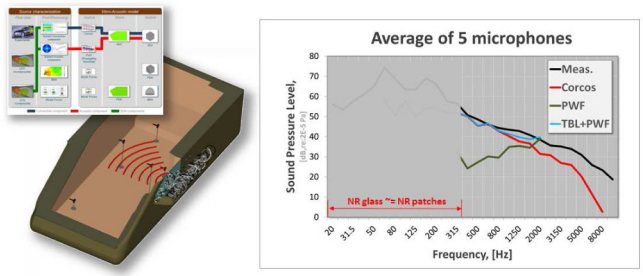

Figure 42. Average SPL inside SAE body generated by 140 km/h wind predicted using a SEA model. Contributions from convective and acoustic component are also shown.

Figure 43 shows the average SPL inside SAE body generated by a 140 km/h wind predicted using the BEM and SEA-FEM-BEM models. The modal forces approach was used. At low frequency, the noise entering the SAE body from all sides contribute to an increase in measured SPL that is not reflected in the predictions since the SAE body walls are considered rigid in the simulation. Correlation between measurements, BEM and SEA-FEM-BEM prediction is high. Computations to higher frequencies are underway.

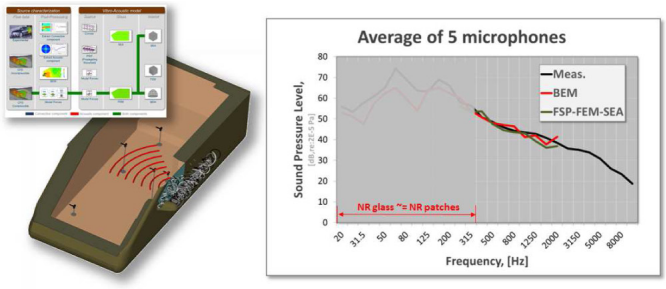

Figure 43. Average SPL inside SAE body generated by 140 km/h wind predicted using a BEM and a FEM/SEA model. The wind noise source is represented by modal forces.

Conclusion

This paper has presented an overview of available methods for characterizing windnoise sources using various approaches. The advantage and disadvantages of these approaches have been discussed and recommendations have been made in relation to when and with which input data these approaches can be the most efficiently used. The validation exercise of the vibro-acoustic model with test data from the SAE body has shown a high degree of correlation confirming that the vibro-acoustics are well modelled. The preliminary Aero-Vibro-Acoustics correlation results are promising and further results for higher frequencies will be published as the become available.

Acknowledgements

The authors would like to thank the CAA German Working Group composed of Audi, Daimler, Porsche and VW for authorizing ESI to use their experimental and CFD data for the VA and AVA validation work presented here [5].

References

1. DeJong, R., Bharj, T., and Lee, J., “Vehicle Wind Noise Analysis Using a SEA Model with Measured Source Levels,” SAE Technical Paper 2001-01-1629, 2001, doi:10.4271/2001-01-1629.
2. DeJong, R., Bharj, T., and Booz, G., “Validation of SEA Wind Noise Model for a Design Change,” SAE Technical Paper 2003-01-1552, 2003, doi:10.4271/2003-01-1552.
3. Peng, G., “SEA Modeling of Vehicle Wind Noise and Load Case Representation,” SAE Technical Paper 2007-01-2304, 2007, doi:10.4271/2007-01-2304.
4. Kralicek, J., Blanchet, D., “Windnoise: Coupling Wind Tunnel Test Data or CFD Simulation to Full Vehicle Vibro-Acoustic Models”, DAGA, Düsseldorf, Germany, 2011.
5. Hartmann, M., Ocker, J., Lemke, T., Mutzke, A. et al., “Wind Noise caused by the A-pillar and the Side Mirror flow of a Generic Vehicle Model”, 18th AIAA/CEAS Aeroacoustics Conference, Paper 2012-2205, Colorado Springs, USA, 2012.
6. Arguillat, B., Ricot, D., Bailly, C., Robert, G., “Measured wavenumber: Frequency spectrum associated with acoustic and aerodynamic wall pressure fluctuations”. JASA 128(4), 2010.
7. Shorter, P., Blanchet, D., and Cotoni, V., “Modeling Interior Noise due to Fluctuating Surface Pressures from Exterior flows,” SAE Technical Paper 2012-01-1551, 2012, doi:10.4271/2012-01-1551.
8. Shorter, P., Cotoni, V., Blanchet, D., “Modeling interior noise due to fluctuating surface pressures from exterior flows”, ISMA, Leuven, Belgium, 2012.
9. Bremner, P., Wilby, J., “Aero-Vibro-Acoustics: Problem Statement And Methods For Simulation-Based Design Solution”, Proc. 8th AIAA/CEAS Aeroacoustics Conference, 2002.
10. VA One 2012, The ESI Group. http://www.esi-group.com
11. Cook, R., et al “Measurement of correlation coefficients in reverberant sound fields”, JASA, 27(6), 1955.
12. Cockburn, J.A., Robertson, J.E., “Vibration Response of Spacecraft Shrouds to In-flight Fluctuating Pressures”, Journal of Sound and Vibration, 1974, 33(4), 399-425.
13. Larko, J.M., Hughes, W.O., “Initial Assessment of the Ares I-X Launch Vehicle Upper Stage to Vibroacoustic Flight Environments”, NASA Technical Memorandum-2008-215167
14. Potschka, N., Callsen, S., “Vibro-acoustic description of a stiffened aircraft structure in flight condition”, ESI Group Vibro-Acoustic User's Conference (VAUC), Düsseldorf, Germany, 2012.
15. Orrenius, U., Cotoni, V., Wareing, A., “Analysis of sound transmission through aircraft fuselages excited by turbulent boundary layer or diffuse acoustic pressure fields”, Internoise, Ottawa, Canada, 2009.
16. Davis, E.B., “By Air by SEA”, Noise-Con, Baltimore, USA, 2004
17. Bremner, P. and Zhu, M., “Recent Progress using SEA and CFD to Predict Interior Wind Noise,” SAE Technical Paper 2003-01-1705, 2003, doi:10.4271/2003-01-1705.
18. Hekmati, A., Ricot, D., Druault, P., “Vibroacoustic behavior of a plate excited by syntesized aeroacoustic pressure fileds”, Proc. 16th AIAA/SEAS Aeroacoustics Conference, AIAA 2010-3950, 2010.
19. Businger, A. Eberle, M. “Computation of underbody flow aero-acoustics for a production vehicle”, ESI Group Global Forum, Munich, Germany 2010
20. Jové, J., Guerville, F., Vallespín, A., “Study Of The Aerodynamic Contribution To The High-Speed Train Cabin Internal Noise By Means Of Hybrid Fe-Sea Modeling”, Internoise, Lisbon, Portugal, 2010.
21. Shorter, P.J., Langley, R.S., and Cotoni, V., “Aeroacoustics: brief review of the theory adopted in VA One”, VAUC/AVA-SIG: Vibro-Acoustic User's Conference & Aero-Vibro-Acoustic Special Interest Group, Düsseldorf, Germany, 2012.
22. Gade, S., Møller, N., Hald, J., Alkestrup, L., “The use of Volume Velocity Source in Transfer Measurements”, Internoise, Prague, Czech Republic, 2004.
23. Luan, Y., Jacobsen, F., “A method of measuring the Green's function in an enclosure”. JASA 123(6), June 2008.
24. Shorter, P.J. and Langley, R.S.: Vibro-acoustic analysis of complex systems, Journal of Sound and Vibration, 2004.

25. Shorter, P.J., and Langley, R.S., “On the reciprocity relationship between direct field radiation and diffuse reverberant loading”. JASA, 117, 85-95, 2005.

Contact Information

D. Blanchet
ESI Group
denis.blanchet@esi-group.com

Definitions/Abbreviations

SEA - Statistical Energy Analysis

BEM - Boundary Element Method

FSP - Fluctuating Surface Pressure: Time domain source type in VA One

TBL - Turbulent Boundary Layer: Corcos model of turbulent flow: Frequency domain source in VA One

PWF - Propagating wavefield: Waves impinging on a panel at a specific angle: Frequency domain source in VA One

FEM - Finite Element Method

DAF - Diffuse Acoustic Field: Random incidence wave field: Frequency domain source in VA One

SPL - Sound pressure level

Corcos - Empirical model describing a complex turbulent flow

FE/SEA Coupled - Method that fully couples FEM and SEA in a unique vibro-acoustic model

VA - Vibro-Acoustics

AVA - Aero-vibro-Acoustics

TBL - Turbulent Boundary Layer: Corcos model: Frequency domain source in VA One

SAE - Society of Automotive Engineers

SAE body - Generic automobile shape

NR - Noise Reduction

CFD - Computational Fluid Dynamics

DES - Detached Eddies Simulation

CAA - Computational Aeroacoustics

$\boldsymbol{k_c}$ - Convective wavenumber, $k_c=\omega/U_c$

$\boldsymbol{k_o}$ - Acoustic wavenumber, $k_o=\omega/U_o$

$\boldsymbol{U_c}$ - Convection velocity

$\boldsymbol{\omega}$ - Angular frequency, $\omega = 2\pi f$

The Engineering Meetings Board has approved this paper for publication. It has successfully completed SAE’s peer review process under the supervision of the session organizer. The process requires a minimum of three (3) reviews by industry experts.

ISSN 0148-7191

http://papers.sae.org/2014-01-2052